ELSEVIER

Computer Networks 39 (2002) 329–345

COMPUTER NETWORKS

www.elsevier.com/locate/comnet

A predictability analysis of network traffic

Aimin Sang *, San-qi Li

Department of Electrical and Computer Engineering, University of Texas at Austin, Engineering Science Building (ENS) 516, Austin, TX 78712-1084, USA

Received 3 November 2001; accepted 12 November 2001

Responsible Editor: I.F. Akyildiz

Abstract

This paper assesses the predictability of network traffic by considering two metrics: (1) how far into the future a traffic rate process can be predicted with bounded error; (2) what the minimum prediction error is over a specified prediction time interval. The assessment is based on two stationary traffic models: the auto-regressive moving average and the Markov-modulated poisson process. In this paper, we do not aim to propose the best traffic (prediction) model, which is obviously a hard and arguable issue. Instead, we focus on the constrained predictability estimation with assumption and discussion about the modeling accuracy. The specific time scale or bandwidth utilization target of a predictive network control actually forms the constraint. We argue that the two models, though both short-range dependent, can capture statistics of (self-similar) traffic quite accurately for the limited time scales of interests in measurement-based traffic management. This argument, in mathematical terms, simply reflects the fact that the summarized exponential (correlation) functions may approximate a hyperbolical one very well.

Our study reveals that the applicability of traffic prediction is limited by the deteriorating prediction accuracy with increasing prediction interval. From both analytical and numerical studies, we explore the different roles of traffic statistics, either at the 1st-order or the 2nd-order, in traffic predictability. Particularly, the statistical multiplexing and proper measurement (e.g. sampling/filtering) of traffic show positive effects. Experimental results suggest promising backbone traffic prediction, and generally enhanced predictability if small time-scale traffic variations, which are usually of less importance to bandwidth allocation and call admission control, have been filtered out. The numerical results in the paper provide quantized reference to the optimal online traffic predictability for network control purposes.

Keywords: Prediction; Time-scale; ARMA; MMPP; Self-similarity

1. Introduction

One of the key issues in measurement-based network control is to predict the bandwidth requirement in the next control time interval based on the online measurement of traffic characteristics. The goal of traffic prediction is to forecast future traffic rate variations as precisely as possible,

* Corresponding author. Tel.: +1-972-461-6272; fax: +1-972-461-7506.

E-mail addresses: asang@santera.com, sang@ece.utexas.edu (A. Sang), sanqi@ece.utexas.edu (S.-q. Li).

1389-1286/02/$ - see front matter
PII: S1389-1286(01)00304-8

based on the measured history. Traffic predictability denotes the possibility for prediction to satisfy some precision requirement over desired prediction/control time interval. On one hand, a large prediction interval is needed to provide sufficient time for control actions, and to offset the inevitable delays caused by traffic measurement (e.g. sampling/filtering) and traffic prediction (modeling/computing). On the other hand, a small prediction error is desirable for the following reason: control actions based on erroneous prediction may inadvertently compromise the control performance. To overcome this problem, one has to be conservative and set aside network resources, specifically the bandwidth resource in this paper. Thus, in order to achieve high resource utilization, a network controller would prefer precise prediction. Unfortunately, prediction accuracy deteriorates quickly as the prediction interval increases. Clearly there is a tradeoff between a large prediction interval and a small prediction error, which reflects the tradeoff between the control time interval and the network efficiency.

Furthermore, traffic of different types have their own inherent nature of predictability. Thus it is important to characterize the dominating traffic statistics in the prediction. The same traffic may show different predictability if looked at different time-scales, i.e. if its rate process is sampled/filtered with different time interval. Therefore, it is critical to understand the measurement impact on predictability and always tie them together. Consequently our major concerns can be summarized into the following questions:

1. How far into the future can network traffic be predicted with confidence requirement? In other words, what is the maximum prediction interval (MPI) under certain error constraint?
2. How much network resource has to be reserved to absorb the prediction uncertainty, if the prediction interval is specified as the network control time interval?
3. What traffic properties, statistically obtained from traffic measurements, characterize its inherent predictability? In addition, how do traffic multiplexing and traffic sampling affect the predictability estimation?

This paper examines all of the above issues. Ideally, if one knows the future traffic changes, a congestion-free network control could be simplified as a dynamic bandwidth allocation according to the prediction results. If the predicted rate exceeds the available bandwidth, either additional bandwidth is needed, or various control mechanisms must be evoked to re-route existing flows, to reduce their source rate by negotiation, or to block new call arrivals. The control time interval strongly depends on individual control mechanism. Generally speaking, it is relatively small for nodal congestion control or dynamic bandwidth allocation, reasonably large for local call admission control (CAC) and substantially larger for (re-)routing. The larger it is, the more the prediction error has to be tolerated through bandwidth over-subscription or reinforced control scheme. Therefore, prediction should meet network control requirements about time-scale and resource utilization target. Inversely, we can evaluate traffic predictability under certain constrains, which comes from the control requirements. The result can be referred for control setup, for example, for the selection of utilization target and its related control time interval.

Some previous works focused on one-step traffic prediction using neural networks [13], or least mean square error (LMSE) derived SNR criterion and adaptive online traffic prediction [1]. Others includes non-stationary signal prediction investigation [8], or a general argument for the enhanced predictability with special 2nd-order traffic property like self-similarity or long-range dependence (LRD) [19,20]. Those studies, in spite of their own advantages, did not show us the efficiency of predictive traffic management, or its numerical potential under practical constraints. We expect to compensate them with this paper by answering the above questions.

Our method is to analyze the quantized multi-step traffic prediction uncertainty, given a complete traffic history and its stationary model as a priori knowledge. Thus, the result provides an upper bound for online prediction performance under specified error constraint or with expected prediction interval. It reveals the promising predictability of network backbone traffic (i.e. aggregated end-system traffic) or low-frequency (LF) (i.e. large time-scale) traffic variations. To answer the question of "Is the traffic predictable?" we need to take into account such factors as the network control time interval, resource utilization target, traffic statistics and the measurement time-scale. In other words, how one assesses traffic predictability depends on how one wants to use the prediction results to meet the control expectation or constraint.

Next are the assumptions underlying our studies. First, we assume that all traffic traces used in this paper are stationary, their characteristics are captured by the 1st- and 2nd-order statistics, i.e. the marginal cumulative distribution function (CDF) and the power spectral density function (PSD). Furthermore, we assume that traffic can be adequately represented by a stationary model such as the auto-regressive moving average (ARMA) or Markov-modulated poisson process (MMPP).

To legitimate our analysis, we assume that the traffic modeling is reasonably accurate. It is well known that self-similarity and LRD are ubiquitous properties of network traffic, including Ethernet [21], MPEG [22] and JPEG [23] video, and WWW [24] traffic. No doubt, fractional Brownian motion (FBM) for exactly self-similar data traffic and fractional ARIMA for asymptotically self-similar video traffic are better models to capture the slowly decaying correlation function and scale-invariant burstiness. However, there are a lot of arguments about whether LRD matters in traffic management for delay-sensitive services. Being supported by [14,25–27], we argue that in a practically mission-critical control environment like ATM network, only limited traffic time-scales concern us. Therefore, ARMA and MMPP models can be used for LRD traffic since their correlation in the form of summarized exponential functions approximate the hyperbolically decaying LRD correlation.

This paper is organized as follows: Section 2 defines the constrained traffic predictability using LMSE-based optimal traffic predictor. Section 3.1 derives ARMA predictability, while Section 3.2 analyzes the effect of traffic measurement (low-pass filtering) and aggregating (multiplexing) on it. Section 3.3 examines the roles of different traffic statistics inherent in predictability. Section 3.4 gives quantitative results for ARMA-matched real traces at proper measurement time-scale and multiplexing level. Section 4 performs the analysis with MMPP model. Section 5 is technical discussion and Section 6 concludes the paper.

2. Definition of traffic predictability

A network traffic is represented by a continuous-time stochastic process $\{Y(t) = X(t) + \mu\}$, where μ is the mean rate, and $\{X(t)\}$ is a purely random (regular) process with continuous integrated spectrum and zero mean. ARMA and MMPP process are all of this form. Ideally, any deterministic components can be extracted from the traffic according to the *Lebesgue decomposition theorem*, and removed from our prediction analysis.

The traffic prediction issue is illustrated in Fig. 1. It depicts the measurement-based control procedure at a finite-buffer network node, whose maximum local delay d_{max} is typically around 30 ms. The queuing process can be characterized by the low pass filter (LPF) with cutoff frequency $1/T_c$ [18,28], i.e. the inverse of the critical time-scale (CTS) [26]. Only the high-frequency (HF) dynamics of the input traffic are absorbed by buffering, whereas the LF part remains unchanged after buffering. Such a T_c can be used as the sampling/smoothing interval for online traffic measurement. Its engineering value ranges from d_{max} to $200d_{max}$ [14]. Thus, the node can be simplified as a "bufferless" transmission system for the filtered input $Y_L(t)$. Its prediction-based network control,

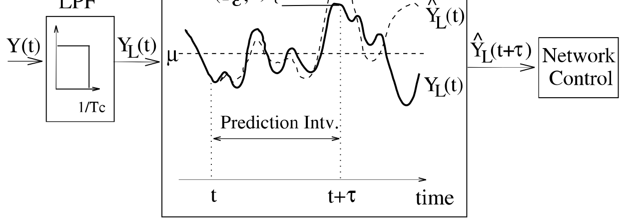

Fig. 1. Traffic prediction framework: $Y(t)$—arrived network traffic, T_c—filtering rate, $Y_L(t)$—filtered traffic rate, μ—traffic mean rate, $(P_\varepsilon, \varepsilon)$—prediction error constraint, $\hat{Y}_L(t+\tau)$—τ-step predictor.

for example the dynamic bandwidth allocation or CAC, requires $Y_L(t+\tau)$ from the measured traffic history $\{Y_L(r)|r \in (-\infty, t]\}$. τ denotes the control or prediction time interval. The result $\hat{Y}_L(t+\tau)$, to be used for control purpose, is named the *τ-step predictor*. For simplicity, we neglect the subscript L in the following notations.

Assume the control requires that the *normalized τ-step prediction error* ($\overline{\text{err}}(\tau) \equiv (\hat{Y}(t+\tau) - Y(t+\tau))/\hat{Y}(t+\tau)$) should not exceed a percentage ε (e.g. 20%) with a probability P_ε (e.g. 0.01), where $(P_\varepsilon, \varepsilon)$ is the desired prediction confidence interval. Then the optimal prediction performance can be characterized by the maximum prediction interval (MPI):

$$\text{MPI} \equiv \max\{\tau | P_{\overline{\text{err}}}(\tau, \varepsilon) \leqslant P_\varepsilon\}, \tag{1}$$

where $P_{\overline{\text{err}}}(\tau, \varepsilon) = \Pr[\overline{\text{err}}(\tau) > \varepsilon]$; $\overline{\text{err}}(\tau)$ is defined from the LMSE-based optimal predictor: $\hat{Y}(t+\tau) = E[Y(t+\tau)|Y(r), -\infty < r \leqslant t]$, which minimizes the *$\tau$-step variance* $\hat{\sigma}_\tau^2$ and maximizes the signal-noise ratio $\text{SNR}(\tau)$, both of which will be introduced below. Obviously a larger MPI implies better predictability. Note that MPI includes both the 1st- and 2nd-order statistics, while an immediate judgement of good predictability upon LRD features may only reflect the 2nd-order property.

If MPI accomodates enough time for measurement, prediction and network control actions, and the MPI-step prediction meets the confident requirement, then the traffic of time granularity T_c would be declared predictable. In other words, the claim is always accompanied by the measurement time interval. An example can show us the physical meanings of the notions: Assume the predictor is taken as dynamically to-be-allocated bandwidth. Then $\overline{\text{err}}(\tau)$ denotes the bandwidth over-subscription percentage (BOSP), while $P_{\overline{\text{err}}}(\tau, \varepsilon)$ can be taken as the bandwidth over-subscription probability (BOSPr). $(P_\varepsilon, \varepsilon)$ is the required utilization target. $\hat{Y}(t+\tau)$ is normalized by the predictor to reflect the over-reserved portion within the allocated bandwidth, which makes more engineering sense. Therefore, once compared with the usually inevitable bandwidth re-negotiation delay, MPI tells the feasibility to achieve the specified network efficiency. From another angle, MPI also denotes the upper bound of the time-scale over which bandwidth allocation can be performed accurately.

Equivalent to the MPI criterion, LMSE-based SNR is another commonly used approach (see [1]) to prediction evaluation: $\text{SNR}(\tau) = E[Y^2(t)]/\hat{\sigma}_\tau^2$, where $\hat{\sigma}_\tau^2$ is the *τ-step variance* of the prediction noise $Y(t+\tau) - \hat{Y}(t+\tau)$, defined by $\hat{\sigma}_\tau^2 = E[(\hat{Y}(t+\tau) - Y(t+\tau))^2]$, Later we will see the engineering advantage of MPI over SNR.

3. Traffic predictability analysis with ARMA model

Gaussian processes are often used to approximate network traffic, especially backbone traffic, where aggregation of a large number of independent sources lends credence to the model. In this section, ARMA model is used to explore the traffic statistical properties dominating the predictability, and to analyze the effect of traffic smoothing and aggregation. After that, quantitative analysis is applied to real network traces.

3.1. Specification of Gaussian predictability

First let us review the conclusions about Gaussian prediction [11]. By *Wold's decomposition theorem*, any stationary regular Gaussian process $\{Y(t) = X(t) + \mu\}$ can be uniquely represented by an one-sided moving average of a stationary Gaussian white noise $\{n(t)\}$ with unit variance:

$$Y(t) = \int_0^{+\infty} h_u n(t-u)\,\mathrm{d}u + \mu, \tag{2}$$

where h_u is a real-valued function of u given a real-valued process $\{Y(t)\}$. The optimal τ-step predictor of the Gaussian process $X(t+\tau)$ is $\hat{X}(t+\tau) = E[X(t+\tau)|X(t-u), 0 \leqslant u < +\infty]$ in the sense of LMSE. This predictor can be expressed as a linear form by stationary Gaussian property (*Wiener's approach*): $\hat{X}(t+\tau) = \int_0^{+\infty} a_u X(t-u)\mathrm{d}u + b$. Equivalently in *Kolmogorov's approach*, $\hat{X}(t+\tau)$ is expressed as:

$$\begin{aligned}\hat{X}(t+\tau) &= \int_\tau^{+\infty} h_u n(t+\tau-u)\,\mathrm{d}u \\ &= \int_0^{+\infty} h_{u+\tau} n(t-u)\,\mathrm{d}u.\end{aligned} \tag{3}$$

A comparison between (2) and (3) tells us that the unpredictable part in $X(t+\tau)$ is $\int_0^\tau h_u n(t+\tau-u)\,\mathrm{d}u$. So the τ-step prediction variance $\hat{\sigma}_\tau^2$ can be expressed as:

$$\hat{\sigma}_\tau^2 = \int_0^\tau h_u^2\,\mathrm{d}u = \sigma^2 - \int_\tau^{+\infty} h_u^2\,\mathrm{d}u, \tag{4}$$

where σ^2 is the variance of $X(t)$. Clearly, $\hat{\sigma}_\tau^2$ is a non-decreasing function of τ. Therefore, the further into the future one tries to predict, the more prediction error one will get. The best prediction of $X(+\infty)$ is its mean and $\hat{\sigma}_\infty^2 = \lim_{\tau\to+\infty}\hat{\sigma}_\tau^2 = \sigma^2$.

Assume the rate process $\{Y(t)\}$ is Gaussian with negligible probability for being negative. From previous definition, we can see that the $P_{\overline{\mathrm{err}}}(\tau,\varepsilon)$ in (1) equals $P(Z>0)$, the tail distribution of a Gaussian variable Z with p.d.f. $N(-\varepsilon\cdot\mu, \sigma_{\varepsilon,\tau}^2)$, where:

$$\sigma_{\varepsilon,\tau}^2 = \int_0^\tau h_u^2\,\mathrm{d}u + \varepsilon^2\int_\tau^{+\infty} h_u^2\,\mathrm{d}u = (1-\varepsilon^2)\hat{\sigma}_\tau^2 + \varepsilon^2\sigma^2. \tag{5}$$

Moreover, according to (3) and (4), $P_{\overline{\mathrm{err}}}(\tau,\varepsilon) \leqslant P_\varepsilon$ in (1) is equivalent to $\sigma_{\varepsilon,\tau}^2 \leqslant (\varepsilon^2\mu^2/\phi^2(1-P_\varepsilon))$. $\phi(x)$ is the inverse CDF of $N(0,1)$. [1] Putting (5) into (1), we can get Gaussian's MPI:

$$\mathrm{MPI} = \max\left\{\tau \left| \frac{\hat{\sigma}_\tau^2}{\sigma^2} \leqslant \mathrm{O}(P_\varepsilon,\varepsilon,C)\right.\right\}, \tag{6}$$

$$\mathrm{O}(P_\varepsilon,\varepsilon,C) = \left[\frac{1}{C^2\phi^2(1-P_\varepsilon)} - 1\right]\frac{\varepsilon^2}{1-\varepsilon^2}, \tag{7}$$

where $C = \sigma/\mu$ is the variance coefficient of $\{Y(t)\}$. Correspondingly from the definition of τ-step SNR, there is:

$$\mathrm{SNR}(\tau)^{-1} = \frac{\hat{\sigma}_\tau^2}{\sigma^2}\cdot\frac{C^2}{1+C^2}, \tag{8}$$

$$\mathrm{MPI} = \max\left\{\tau \left| \mathrm{SNR}(\tau)^{-1} \leqslant \frac{|\mathrm{O}(P_\varepsilon,\varepsilon,C)\cdot C^2}{1+C^2}\right.\right\}. \tag{9}$$

Take a look at (6) and (7). Although the normalized prediction variance $\hat{\sigma}_\tau^2/\sigma^2$ falls into $[0,1]$, the τ-independent $\mathrm{O}(P_\varepsilon,\varepsilon,C)$ can be negative when $C > 1/(\phi^2(1-P_\varepsilon))$ or larger than 1 upon a sufficiently large ε. In other words, MPI can be 0 upon large traffic varying amplitude (C) or stringent BOSP (P_ε), and be $+\infty$ upon a large error tolerance (ε). Obviously traffic predictability is a function of both the confidence requirement (P_ε, ε), and the 1st- and 2nd-order statistics. It is decided by the comparison between P_ε and $P_{\overline{\mathrm{err}}}$, i.e. the tail distribution of $N(-\varepsilon\cdot\mu, \sigma_{\varepsilon,\tau}^2)$, whereas the 2nd-order traffic statistics exert influence through $\hat{\sigma}_\tau^2$. However, $\lim_{\tau\to+\infty} P_{\overline{\mathrm{err}}}(\tau,\varepsilon) = \Pr[Y(t) < (1-\varepsilon)\mu]$. That is, the prediction effect of the infinite future is exclusively determined by the traffic tail distribution.

3.2. *Effects of (low-pass) filtering and multiplexing on traffic predictability*

In practice, traffic rate sampling (i.e. low-pass filtering) and multiplexing play critical roles in measurement-based network control or traffic engineering. Here we check their influence on traffic predictability. First, assume $\{X(t) = Y(t) - \mu\}$ can be decomposed into $L\,(>1)$ mutually independent components: $\{X(t)\} = \sum_{l=1}^{L}\{X_l(t)\}$. Each component is still a stationary Gaussian process. A commonly used decomposition method is to filter the traffic into non-overlapping frequency regions using an ideal band-pass filter. In time domain, this corresponds to the traffic dissection at multiple time-scales. Some may argue that the decomposed processes are not regular, but they can always be transferred into regular ones by removing their deterministic components, according to *Lebesgue decomposition theorem*. The next two propositions analytically state the predictability changes after this kind of operation.

[1] Though modeling error is not our major concern in the paper, we can still roughly remove the possibly non-negligible occurrence of negative $\hat{Y}(t+\tau)$ by adding a condition $\hat{Y}(t+\tau) \geqslant 0$ to $P_{\overline{\mathrm{err}}}(\tau,\varepsilon)$. Then $P_{\overline{\mathrm{err}}}(\tau,\varepsilon) \leqslant P_\varepsilon$ is equivalent to:

$$\frac{1}{1-\Phi\left(\frac{-\mu}{\sqrt{1-\hat{\sigma}_\tau^2}}\right)}\int_{-\mu/\left(\sqrt{1-\hat{\sigma}_\tau^2}\right)}^{+\infty}\Phi\left(-z\varepsilon\sqrt{\frac{1}{\hat{\sigma}_\tau^2}-1}-\frac{\varepsilon\mu}{\sqrt{\hat{\sigma}_\tau^2}}\right)\times f(z)\,\mathrm{d}z \leqslant P_\varepsilon,$$

where $\Phi(*)$ is the CDF of $N(0,1)$ and $f(z)$ is the distribution density function of $Z\sim N(0,1)$.

Proposition 1. *Denote the τ-step prediction variance of $\{X(t)\}$ and $\{X_l(t)\}$ as $\hat{\sigma}^2_\tau$ and $\hat{\sigma}^2_{l,\tau}$ respectively. Then the prediction variance of $\{X(t)\}$ is not smaller than the sum of that of all $\{X_l(t)\}$: $\hat{\sigma}^2_\tau \geqslant \sum_l \hat{\sigma}^2_{l,\tau}, \forall\tau$.*

Proof. By *Wiener's approach*, the optimal τ-step predictor of $X(t+\tau)$ is:

$$\hat{X}(t+\tau) = E[X(t+\tau)|X(t-u), 0 \leqslant u < +\infty] = \int_0^{+\infty} a_u X(t-u)\,\mathrm{d}u + b.$$

To minimize the τ-step prediction variance $\hat{\sigma}^2_\tau$ as required by the LMSE criterion, the optimal parameters $a_u(\forall u)$ and b satisfy the well-known *Wiener–Hopf equations*: $\forall v \in [0, +\infty]$,

$$\int_0^{+\infty} C_X(t-u, t-v) a_u\,\mathrm{d}u = C_X(t+\tau, t-v),$$

$$b = E[X(t+\tau)] - \int_0^{+\infty} a_u E[X(t-u)]\,\mathrm{d}u = 0,$$

where $C_X(\cdot, \bullet)$ is the auto-correlation function of $\{X(t)\}$. Due to the optimal a_u and b and the fact that $E[(X(t+\tau) - \hat{X}(t+\tau))\hat{X}(t+\tau)] = 0$, the minimized $\hat{\sigma}^2_\tau$ is:

$$\hat{\sigma}^2_\tau = \sigma^2 - \int_{u=0}^{+\infty} \int_{v=0}^{+\infty} C_X \times (t-v, t-u) a_v a_u\,\mathrm{d}v\,\mathrm{d}u. \tag{10}$$

In fact this equation also holds for every $\{X_l(t)\}$ with corresponding $\hat{\sigma}^2_{l,\tau}$, σ^2_l, $C_{X_l}(\cdot, \bullet)$ and $(a_{l,u}, b_l)$. [2] Because of the independent decomposition, it follows:

$$\sigma^2 = \sum_{l=1}^{L} \sigma^2_l \quad \text{and} \quad C_X(\cdot, \bullet) = \sum_{l=1}^{L} C_{X_l}(\cdot, \bullet).$$

Therefore,

$$\begin{aligned}
\hat{\sigma}^2_\tau &= \sum_{l=1}^{L} \left(\sigma^2_l - \int_{u=0}^{+\infty} \int_{v=0}^{+\infty} C_{X_l}(t-v, t-u) a_u a_v\,\mathrm{d}v\,\mathrm{d}u \right) \\
&\geqslant \sum_{l=1}^{L} \left(\sigma^2_l - \int_{u=0}^{+\infty} \int_{v=0}^{+\infty} C_{X_l}(t-v, t-u) a_{u,l} a_{v,l}\,\mathrm{d}v\,\mathrm{d}u \right) \\
&= \sum_{l=1}^{L} \hat{\sigma}^2_{l,\tau},
\end{aligned}$$

because it is $(a_{u,l}, a_{v,l})$, instead of (a_u, a_v), uniquely minimizes $\hat{\sigma}^2_{l,\tau}$. If the decomposition is i.i.d., then we can show that $\forall\tau$, $\hat{\sigma}^2_\tau = \sum_{l=1}^{L} \hat{\sigma}^2_{l,\tau}$. □

Proposition 2. *Denote the MPI of $\{Y(t) = X(t) + \mu\}$ and $\{Y_l(t) = X_l(t) + \mu\}$ as τ^* and τ^*_l respectively, within the same prediction confidence interval $(P_\varepsilon, \varepsilon)$. Then the MPI of $\{Y(t)\}$ is not larger than the minimum one among MPIs of all $\{Y_l(t)\}$: $\tau^* \leqslant \min_l \tau^*_l$.*

Proof. Assume $\tau^* > \tau^*_l$. For the optimal prediction of a Gaussian process from a complete history, $\hat{\sigma}^2_\tau$ is a non-decreasing function of τ. With the conclusion of Proposition 1, we can get: $\hat{\sigma}^2_{\tau^*} \geqslant \hat{\sigma}^2_{l,\tau^*} \geqslant \hat{\sigma}^2_{l,\tau^*_l}$. However, by (6) and (7), $\hat{\sigma}^2_{\tau^*} \geqslant \hat{\sigma}^2_{l,\tau^*_l}$ implies $\sigma^2 \leqslant \sigma^2_l$, which is surely impossible. □

Proposition 1 tells us that the prediction of a purely random (Gaussian) process is not better than that of any of its independently-decomposed components. Proposition 2 suggests that the (ideal) low-pass filtering, which keeps traffic mean rate intact, improves the predictability. Intuitively, a LPF slows down traffic changes by removing small time-scale variations (HF randomness) from the traffic, thus brings a more predictable traffic behavior. The more randomness one filters out, the better result one can get. In an extreme case, if only the DC term μ were left after filtering, it would have an unlimited predictability.

Next we will check the effect of traffic statistical multiplexing on its predictability. Assume $\{Y(t)\}$ is the superposition of M i.i.d. Gaussian processes $\{Y_m(t) = X(t) + \mu\}$ $(m = 1, 2, \ldots, M)$. After the aggregation, the $\mathrm{O}(P_\varepsilon, \varepsilon, C)$ in Eq. (7) increases because C^2 is scaled up with M. However, $\hat{\sigma}^2_\tau/\sigma^2$ remains unchanged because $\hat{\sigma}^2_\tau$ and σ^2 increase with the same scale by (4). Therefore, it can be seen clearly from (6) that traffic multiplexing increases MPI, and thus improves predictability. This fact reveals that generally a better prediction can be expected for aggregated traffic sources, compared to that for each individual one. In addition, a high-level multiplexing (i.e. a big M) can make the $\mathrm{O}(P_\varepsilon, \varepsilon, C)$ larger than one by scaling down C. If so, the aggregated source would have an unlimited predictability in the sense that the prediction of its

[2] Please note that the $C_X(\cdot, \bullet)$ and $C_{X_l}(\cdot, \bullet)$ here are independent of t for their stationarity, whereas (a_u, b) and $(a_{l,u}, b_l)$ are functions of τ.

any future would never violate the $(P_\varepsilon, \varepsilon)$ requirement.

Although not proved, we believe that the above conclusions also hold for a self-similar traffic. The traffic, if investigated at limited but meaningful time-scales, may be predicted more easily than at all time-scales simultaneously. On the other hand, multiplexing reduces the traffic fluctuation amplitude around its mean rate, i.e. even if the 2nd-order burstiness (denoted by a *Hurst parameter* larger than 0.5) remains similar. Later the conclusions will be verified by quantitative analysis of real traffic traces.

3.3. Roles of traffic properties in traffic predictability

What traffic properties characterize the inherent traffic predictability? By [16,17], traffic statistics of orders higher than two has little effect on queuing performance. Therefore, we will use the Gaussian traffic process of a bell-shaped power spectrum for analysis in that it provides a decomposable statistical structure.

With this help, we first show that the half-power PSD bandwidth plays a more fundamental role in determining traffic predictability than other 2nd-order statistics, such as the central frequency of PSD bells. In other words, the PSD spectrum dispersion has more side effect on predictability than the PSD frequency location. In time domain, it is identical to the number of traffic correlation time-scales verse specific time-scale sizes. The more time-scales a traffic process is correlated at, the harder it can be predicted. This holds no matter whether the time-scales are all big or all small. Induced from this point, the correlation time-scale abundance across a wide range, as a property of most network traffics, has a negative effect on predictability.

Furthermore, we find that a narrow-banded traffic is relatively easier to predict, and wide-banded PSD components contribute more to the total prediction error. Thus, LRD traffic, corresponding to the one of narrow-banded PSD that follows the power law when approximating zero frequency, tends to be easier to predict than short-range dependence (SRD) traffic. The SRD component of a traffic is the main hurdle to its good predictability.

Finally, we show that among the 1st-order traffic statistics, the CDF tail behavior accounts the most for traffic predictability, while the variance coefficient reflects predictability in a straightforward way. The analysis follows.

Assume the power spectrum and auto-correlation function of $\{Y(t)\}$ are respectively [16]:

$$P(\omega) = 2\pi\mu^2\delta(\omega) + \sum_{l=1}^{N-1} \frac{\psi_l(-2\lambda_l)}{\lambda_l^2 + \omega^2},$$

$$R(t) = \mu^2 + \sum_{l=1}^{N-2} \psi_l \mathrm{e}^{\lambda_l |t|},$$

where N is the eigenvalue number; μ^2 is the DC-term of a zero eigenvalue; ψ_l is the corresponding power vector of eigenvalue λ_l. Each pair of (ψ_l, λ_l) forms a bell-shaped component in PSD. Each bell has a half-power PSD bandwidth $\mathrm{BW}_l = -2\mathrm{Re}(\lambda_l)$ and central frequency $\omega_l = \mathrm{Im}(\lambda_l)$. From the *canonical factorization* of PSD, we can get the unique transfer function of the ARMA process as $H(s) = \int_0^{+\infty} h_u \mathrm{e}^{-su}\,\mathrm{d}u$, which is equivalent to $X(t) = \int_0^{+\infty} h_u n(t-u)\,\mathrm{d}u$. Then $\hat{\sigma}_\tau^2$ can be derived from (4).

For simplicity, let us consider the prediction of an ARMA(2,1) process with the assumption of $\lambda_1 = \lambda_2^* \equiv \lambda \mathrm{e}^{j\omega}$ and $\psi_1 = \psi_2^* \equiv \psi \mathrm{e}^{j\beta}$. After a complex PSD factorization, we get:

$$\frac{\hat{\sigma}_\tau^2}{\sigma^2} = 1 - \mathrm{e}^{-\mathrm{BW}\tau} + \mathrm{e}^{-\mathrm{BW}\tau}\left[1 + \sin(2\omega\tau)\tan\beta - \cos(2\omega\tau) - \frac{1-\cos(2\omega\tau)}{\cos\beta\left(\cos\beta + \sqrt{(\frac{\mathrm{BW}}{2\lambda})^2 - \sin^2\beta}\right)}\right], \quad (11)$$

where $\sigma^2 = 2\psi\cos\beta$ is the variance of the process. A numerical study tells us that the PSD bell bandwidth (BW), central frequency (ω) and phase (β) have similar roles in predictability as in auto-correlation function $R(\tau) = 2\psi \mathrm{e}^{-(\mathrm{BW}/2)|\tau|}\cos(\omega|\tau| + \beta)$.

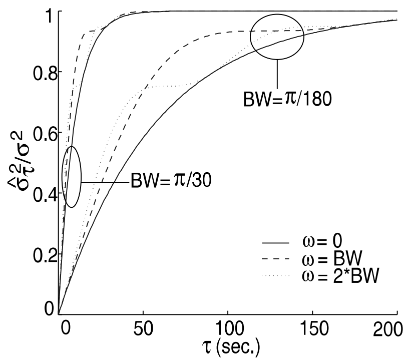

Fig. 2. Normalized prediction variance as a function of τ.

To some extent, $R(\tau)$ characterizes traffic predictability if the 1st-order statistics are fixed.

Using the ARMA(2,1) as an example, Figs. 2 and 3 illustrate the roles of BW, ω and C in its predictability with $\beta = 0$ for simplicity. It is obvious that $\hat{\sigma}_\tau^2/\sigma^2$ increases with τ, reflecting more prediction uncertainty over larger prediction interval. BW denotes the exponentially decaying rate of traffic predictability, and ω represents its oscillation frequency. In frequency domain, it is the PSD bandwidth, not the central frequency, that dominates traffic predictability. In another viewpoint, a wide PSD bandwidth implies large spectrum dispersion, thus abundant traffic randomness, and consequently poor traffic predictability. In extreme cases, a white noise which has an infinite BW and zero MPI, or a sinusoidal process which has a zero BW and an infinite MPI, makes the argument intuitive. In addition, as illustrated by Fig. 3(b), a small C, coming from a big mean (1st-order) or a small variance (2nd-order), reflects a smooth traffic, and therefore better predictability. In the figure, 0.086 is the lower bound of C to ensure $O(P_\varepsilon, \varepsilon, C)$ less than one.

Take aggregated voice sources for example. Each voice source can can be characterized by an on-off model whose average talkspurt and silence period are 0.4 and 0.6 s respectively [4]. The input rate during talkspurt period is 32 Kbps (i.e. 75.5 cells/s). A T1 link with a 300-cell buffer can support 98 voice channels with average cell loss rate less than 10^{-5}. It is calculated by solving the finite quasi-birth–death (QBD) distribution for the T1 queuing system using the Folding algorithm [15]. The superposition of M i.i.d. voice sources (an MMPP process) has a single-bell PSD of $(\mathrm{BW}, \omega) = (2(1/0.4 + 1/0.6), 0)$ and $C = \sqrt{0.6/0.4M}$. Detailed derivations can be referred to [16]. In addition, the aggregate source can be approximated by a first order ARMA process, especially when M is big (98, say). From *canonical factorization* and (6), we get:

$$\frac{\hat{\sigma}_\tau^2}{\sigma^2} = 1 - e^{-\mathrm{BW}\tau}, \quad \mathrm{MPI} = \frac{1}{(-\mathrm{BW})} \ln[1 - O(P_\varepsilon, \varepsilon, C)].$$

The MPI is depicted in Fig. 4(a), where the dotted lines denote the upper limits of M to make $O(P_\varepsilon, \varepsilon, C)$ equal to one, and MPI infinity. For example, when $(P_\varepsilon, \varepsilon)$ is (0.01, 20%), MPI = [29, 156, 770 ms] for $M = [50, 150, 203]$. However, MPI is infinity as $M \geqslant 204$. Furthermore, if $(P_\varepsilon, \varepsilon)$ is relaxed from (0.01, 20%) to (0.1, 20%), we get MPI = [76, 599 ms] for M = [30, 61], and MPI is infinity for $M \geqslant 62$. The intuition behind this is: for a high degree of traffic aggregation, or a loose error constraint, the prediction scheme reduces to the estimation of the deterministic mean rate, which

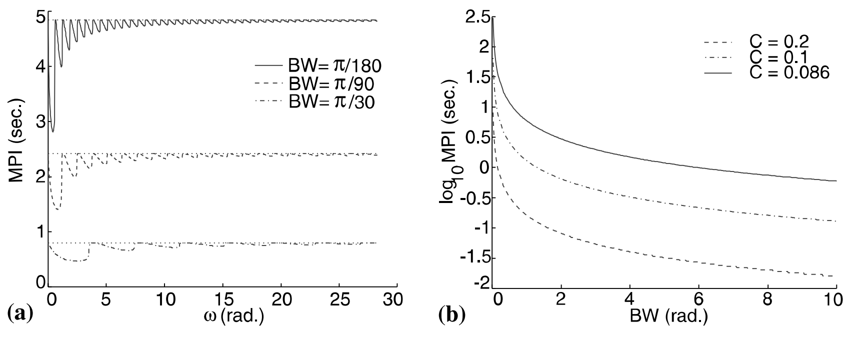

Fig. 3. Effect of PSD factors and C on MPI at $(P_\varepsilon, \varepsilon) = (0.01, 20\%)$: (a) $C = 0.25$, (b) $\omega = 0$.

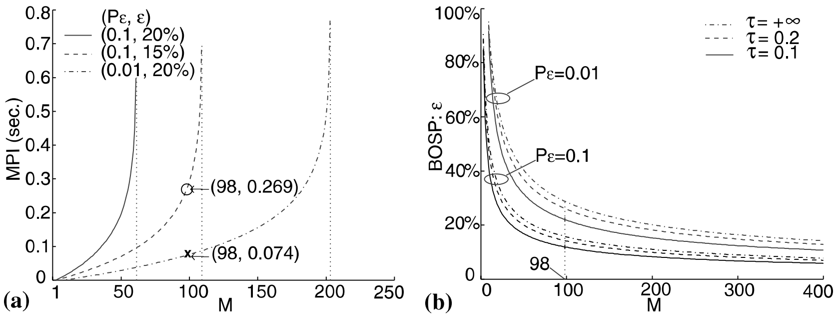

Fig. 4. ARMA prediction of M i.i.d. multiplexed Voice channels: (a) predictability, (b) ε: $\Pr[\overline{\mathrm{err}}(\tau) > \varepsilon] = P_\varepsilon$.

results in an infinite MPI. The two points ("$\circ$" and "$\times$") in the figure shows that for the T1 system, prediction interval of the aggregated voice channels can not be larger than 269 or 74 ms with the confidence interval of (0.1, 15%) or (0.01, 20%) respectively. It means that we can not confidently predict the rate of next talkspurt, not even for the aggregate source! We can, however, confidently predict the infinite future if $(P_\varepsilon, \varepsilon)$ is relaxed to (0.1, 20%)! On the other hand, if 1 s's future is to be predicted, only the right regions to the M limits (see Fig. 4(a)) are "predictable" for corresponding confidence requirements. Nevertheless, the results here are for unfiltered voice traffic.

Fig. 4(b) shows the $(1 - P_\varepsilon)$-percentile limit of prediction error, i.e. the upper bound of the bandwidth resource set aside (as BOSP) to absorb the error: With probability P_ε, $\overline{\mathrm{err}}(\tau)$ may exceed its limit ε. Equivalently, with probability $1 - P_\varepsilon$, ε upper bounds the reserved bandwidth resource (BOSP). In other words, prediction-based network control can expect a higher bandwidth utilization (1−BOSP) with increasing aggregation level (M).

3.4. Predictability studies for real traffic traces

In this section, we analyze the predictability of some real network traces sampled and aggregated at different scales. A sliding window of size T_c is used as the LPF for traffic sampling, where T_c takes empirical engineering values. Prony method [10], which works well with the absence of noise, is used to estimate and identify an ARMA process for the sampled traffic traces. Consequently, $\hat{\sigma}_\tau^2$ and MPI can be obtained from (4) and (7) respectively. The 99-percentile traffic predictability, i.e. with P_ε fixed as 0.01, is presented. The numerical results verify previous analysis, and show upper bounds for the optimal performance of online prediction.

The traces used here are Internet [5], Ethernet [2], MPEG-1 [12] and JPEG [6], with very different characteristics by reference. The Internet is the Fixwest trace of a length 1084 s and a mean rate 26.32 Mbps. The Ethernet is the LAN traffic (BC-pAug89) of 3142.83 s and 1.105 Mbps respectively. The MPEG-1 is a Starwar video trace of 3600 s and 0.334 Mbps. The JPEG is a segment (the slice 10–19) of Starwar video trace of 1187 s and 5.272 Mbps. The variance coefficient is shown in (a)'s of Figs. 5–8 respectively. To get a good match (of the LF PSD especially), the ARMA model's order is selected carefully. For instance, the Internet trace is well matched by ARMA(23,22), ARMA(15,14) and ARMA(3,2) when $T_c = 1$, 4 and 10 s respectively. The higher order reflects more exponential components needed to capture the more traffic correlation time scales because of the finer sampling granularity.

From the (a)'s of Figs. 5–8, we can see clearly that larger traffic (measurement) time-scale derives better predictability. In addition, $\hat{\sigma}_\tau^2/\sigma^2$ monotonically increases with τ, reflecting the deteriorating prediction precision with expanding prediction interval. The MPI of single trace is shown in Table 1, where 0.01 represents the numerical precision, and 0 occurs when $O(P_\varepsilon, \varepsilon, C)$ in (6) is negative. By the numbers, the predictability of end-system traffics, such as the Ethernet, JPEG and MPEG-1, is not encouraging in that their MPIs are even less than the sampling interval! In other words, we

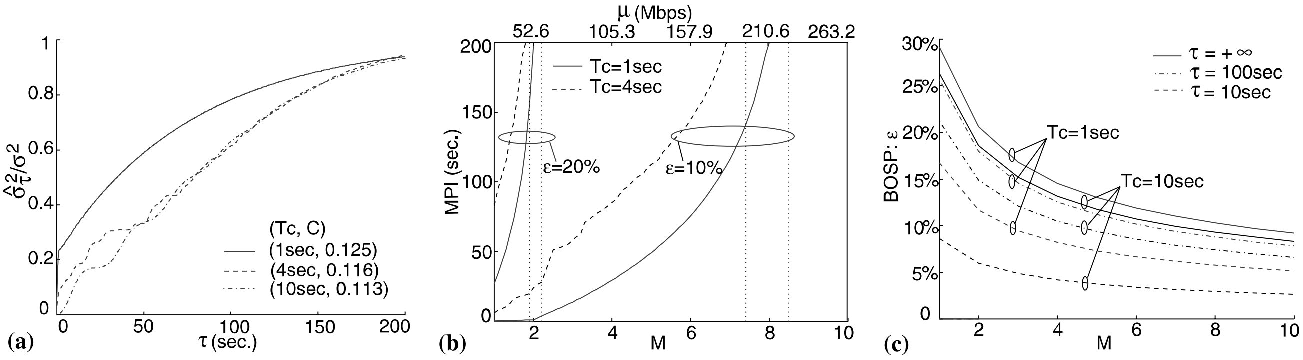

Fig. 5. ARMA-matched Internet trace: (a) normalized prediction variance, (b) MPI, (c) ε: $\Pr[\overline{\mathrm{err}}(\tau) > \varepsilon] = P_\varepsilon$.

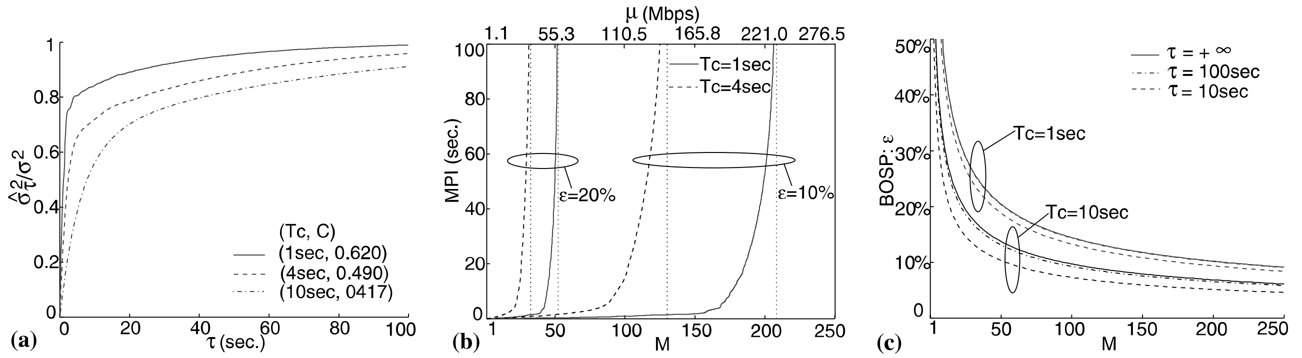

Fig. 6. ARMA-matched Ethernet trace: (a) normalized prediction variance, (b) MPI, (c) ε: $\Pr[\overline{\mathrm{err}}(\tau) > \varepsilon] = P_\varepsilon$.

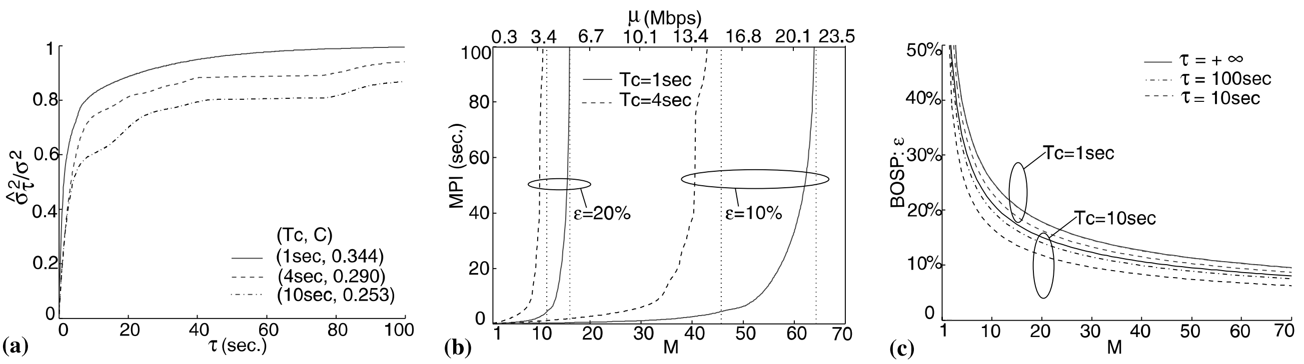

Fig. 7. ARMA-matched MPEG-1 trace: (a) normalized prediction variance, (b) MPI, (c) ε: $\Pr[\overline{\mathrm{err}}(\tau) > \varepsilon] = P_\varepsilon$.

cannot even confidently predict the next step of the sampled traces, even all of them have a self-similar structure. Although contrary to our expectation, we believe it is a natural result from the prediction definition as a function of C, the 2nd-order correlation statistics, and the tight confidence interval with practical engineering and control meanings. For Ethernet, its CSMA/CD mechanism and the unpredictable source interaction may explain this. For JPEG and MPEG-1 video, the bursty scene changes and the non-stationary pseudo-periodic (MPEG I-B-P) frame size variations account for the poor online predictability. Comparatively, JPEG exhibits better predictability than MPEG-1 and Ethernet, as implicitly indicated by its smaller C and thus a smoother behavior.

In contrast, Internet prediction has much better results for the multiplexing gain, therefore im-

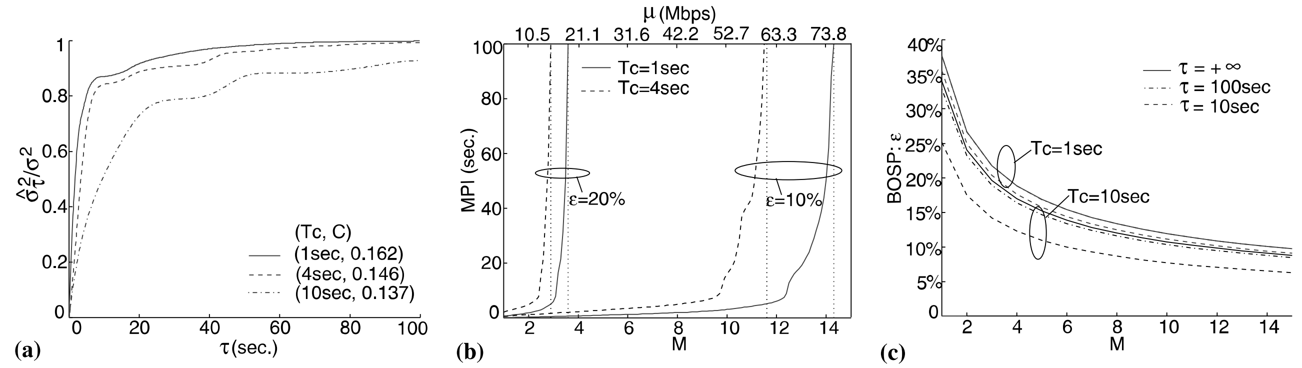

Fig. 8. ARMA-matched JPEG trace: (a) normalized prediction variance, (b) MPI, (c) ε: $\Pr[\overline{\mathrm{err}}(\tau) > \varepsilon] = P_\varepsilon$.

Table 1
ARMA-based MPI (s) for single trace, $P_\varepsilon = 0.01$

ε	T_c (s)	MPEG-1	JPEG	Ethernet	Internet
10%	1	*0.01*	*0.12*	*0*	*0.41*
	4	*0.05*	*0.57*	*0*	6.09
	10	*0.08*	*0.88*	*0.01*	12.79
20%	1	*0.04*	*0.67*	*0*	27.08
	4	*0.21*	*2.09*	*0*	83.03
	10	*0.35*	*5.54*	*0.05*	89.68

Table 2
ARMA-based MPI (s) for i.i.d. multiplexed traces, $(P_\varepsilon, \varepsilon) = (0.01, 10\%)$

Load level	T_c (s)	MPEG-1	JPEG	Ethernet	Internet
Mean at OC-1	1	$+\infty$	3.08	*0.59*	1.22
	4	$+\infty$	16.04	*1.37*	24.18
	10	$+\infty$	$+\infty$	*7.60*	39.96
Mean at OC-3	1	$+\infty$	$+\infty$	1.61	75.94
	4	$+\infty$	$+\infty$	$+\infty$	144.89
	10	$+\infty$	$+\infty$	$+\infty$	160.83

plies more potential usage in reality. As further proved by the (b)'s of Figs. 5–8, traffic aggregation improves traffic predictability, where MPI are obtained for M i.i.d. multiplexed sources while prediction error is limited by $(P_\varepsilon, \varepsilon)$. For each specified T_c and ε, the dotted line denotes the limit of M to reach an infinite MPI.

Usually we are more interested in the predictable time-scale of aggregated traces in real scenarios, where link speed allows reasonable level of traffic multiplexing. Table 2 presents this with the MPI of i.i.d. multiplexed traces at OC-1 and OC-3 link level. It is observed that at reasonable aggregation level, pure MPEG-1 or JPEG also demonstrates good predictability. The Internet and Ethernet has poorer predictability simply because of the less multiplexing gain for smaller source numbers. Generally speaking, much better predictability can be expected for network backbone traffic that bears heavily multiplexed end-system sources, in contrast to a single end-system traffic source. Still, the sampling interval plays a crucial role in the assessment.

The (c)'s of Figs. 5–8, depict the upper bound (ε) of the prediction error ($\overline{\mathrm{err}}(\tau)$) as before. They demonstrate the tradeoff between small BOSP (i.e. small bandwidth loss) and large control interval. In Fig. 5(c) for example, assume $\varepsilon = 30\%$ is an affordable utilization loss, the prediction-based Internet traffic engineering would be feasible for the remotest future. Usually, per-flow traffic prediction is too costly to benefit control purposes. Therefore, it has more limited usage than aggregated traffic prediction. Yet, a carefully selected T_c may help both cases.

To get more insights to our predictability criterion MPI, we calculate the BOSP and the inverse SNR for 1-step traffic prediction in Table 3. As we discussed before, MPI and SNR are two equivalent criteria in the sense of LMSE. The table shows the lower bounds of online prediction noise from two different angles. Network controller may select either one for evaluation. However, we can see clearly from the table that the small SNR^{-1} actually gives an over-optimistic, if not misleading, impression about online traffic predictability. The

Table 3
ARMA-based 1-step ($\tau = T_c$) prediction error for single trace

Error measure	T_c (s)	MPEG-1	JPEG	Ethernet	Internet
BOSP	1	65.1%	23.1%	376.8%	15.5%
	4	55.9%	26.6%	128.2%	9.4%
	10	49.3%	23.5%	95.1%	8.6%
SNR^{-1}	1	0.043	0.009	0.156	0.004
	4	0.042	0.012	0.115	0.002
	10	0.036	0.010	0.083	0.001

next example shows how the BOSP and SNR^{-1} form the bounds of the optimal online prediction performance: In paper [1], the adaptive LMSE approach is used to predict the 1-step GOP rate of the Starwar MPEG video in real time. The value of SNR^{-1} was computed as 0.068 in that paper. It is larger than the lower bound (0.043) given in our table, where ARMA prediction is armed with a complete traffic history and stationarity assumption as well. On the other hand, if $\varepsilon = 10\%$ and set 0.068 as the maximum SNR^{-1}, MPI would be 2.95 s by (6) and (8). This value is surely an upper bound of the one-step ($\tau = 1$ s) prediction interval in [1].

4. Traffic predictability analysis with MMPP model

Up to now, we have examined traffic predictability using ARMA model. Will the conclusions be consistent if the MMPP is used instead? By our previous research [17], circulant Markov-modulated poisson process (CMPP) being a special MMPP can be used to match real traces. It captures not only the 2nd-order statistics, just as ARMA does, but also the 1st-order statistics even of a non-Gaussian distribution. This model performs well in queuing analysis by our previous research [17].

4.1. Specification of CMPP predictability

First take a look at the CMPP properties [17]. CMPP process $\{Y(t)\}$ has a rate vector $\vec{r} = [r_1, \ldots, r_i, \ldots, r_N]$ and a N-state circulant transition matrix Q. The steady-state probability of this process is $1/N$ for all states. In addition, there is the decomposition of $Q = \mathbf{F}\Lambda\mathbf{F}^*$, where $\mathbf{F}$ is a Fourier matrix with the (i,j)th element as $W^{ij} = \frac{1}{\sqrt{N}}\mathrm{e}^{(-2\pi(i-1)(j-1)/N)\sqrt{-1}}$, $\mathbf{F}^*$ is the conjugate transpose of $\mathbf{F}$, and $\Lambda = \mathrm{diag}[\lambda_1, \ldots, \lambda_i, \ldots, \lambda_N]$. All eigenvalues in Λ have a negative real part except $\lambda_1 = 0$. Assume $Y(t) = r_i$, then the probability for $Y(t+\tau) = r_j$ should be $[\mathrm{e}^{Q\tau}]_{ij}$, i.e. the (i,j)th element of the transition probability matrix $[\mathrm{e}^{Q\tau}]$.

By Markov property, the optimal predictor for $Y(t+\tau)$ is:

$$\begin{aligned}\hat{Y}_i(t+\tau) &\equiv E[Y(t+\tau)|Y(t) = r_i] \\ &= \sum_{k=1}^{N} r_k[\mathrm{e}^{Q\tau}]_{ik} \\ &= \frac{1}{N}\sum_{k=1}^{N} r_k \sum_{l=1}^{N} \mathrm{e}^{\lambda_l\tau} W^{l(i-k)}. \end{aligned} \tag{12}$$

Therefore a conditional BOSPr, the prediction error probability subject to the initial state of $Y(t) = r_i$, can be written as:

$$P_{\overline{\mathrm{err}}_i}(\tau, \varepsilon) = \Pr[\overline{\mathrm{err}}_i(\tau) > \varepsilon | Y(t) = r_i] = \sum_{\{j\}_i^*} [\mathrm{e}^{Q\tau}]_{ij},$$

where $\{j\}_i^* = \{j | r_j < (1-\varepsilon)\hat{Y}_i(t+\tau)\}$, and $\overline{\mathrm{err}}_i(\tau) = (\hat{Y}_i(t+\tau) - Y(t+\tau)/\hat{Y}_i(t+\tau))$. By (1), the $(1-P_\varepsilon)$-percentile CMPP predictability is:

$$\mathrm{MPI} = \max\{\tau | P_{\overline{\mathrm{err}}}(\tau, \varepsilon) < P_\varepsilon\}, \quad \text{where}$$
$$P_{\overline{\mathrm{err}}}(\tau, \varepsilon) = \frac{1}{N}\sum_{i=1}^{N} P_{\overline{\mathrm{err}}_i}(\tau, \varepsilon) = \frac{1}{N}\sum_{i=1}^{N}\sum_{\{j\}_i^*} [\mathrm{e}^{Q\tau}]_{ij}. \tag{13}$$

$P_{\overline{\mathrm{err}}}(\tau, \varepsilon)$ is the steady-state BOSPr for predicting $Y(t+\tau)$ from $Y(t)$. By (12), there is $\forall i$, $\lim_{\tau\to+\infty} \hat{Y}_i(t+\tau) = \mu$. Furthermore, $\lim_{\tau\to+\infty} P_{\overline{\mathrm{err}}}(\tau, \varepsilon) = \lim_{\tau\to+\infty} P_{\overline{\mathrm{err}}_i}(+\tau, \varepsilon) = \Pr[Y(t) < (1-\varepsilon)\mu]$. Therefore, prediction performance of the infinite future again depends only on the 1st-order statistics of the traffic.

When M MMPP sources $(Q_m, \vec{r}_m)(m = 1, 2, \ldots, M)$ are multiplexed together, the aggregate source is also an MMPP with $(Q, \vec{r})$ given by:

$$Q = Q_1 \oplus Q_2 \oplus \cdots \oplus Q_M, \quad \vec{r} = \vec{r}_1 \oplus \vec{r}_2 \oplus \cdots \oplus \vec{r}_M,$$

where $\oplus$ is the Kronecker sum operator. However, the state number of the aggregate source may ex-

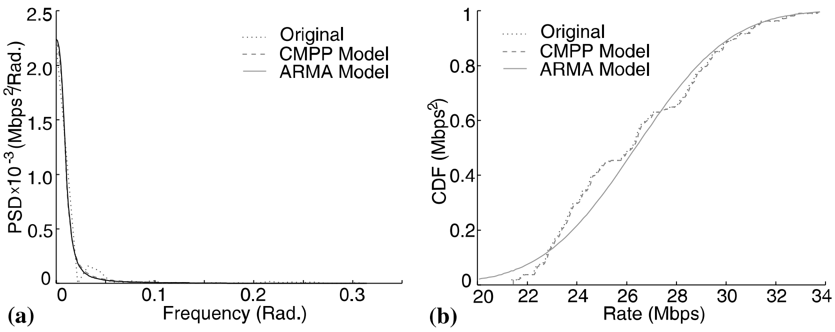

Fig. 9. The matching effect of the Internet trace, $T_c = 10$ s: (a) PSD matching (b) CDF matching.

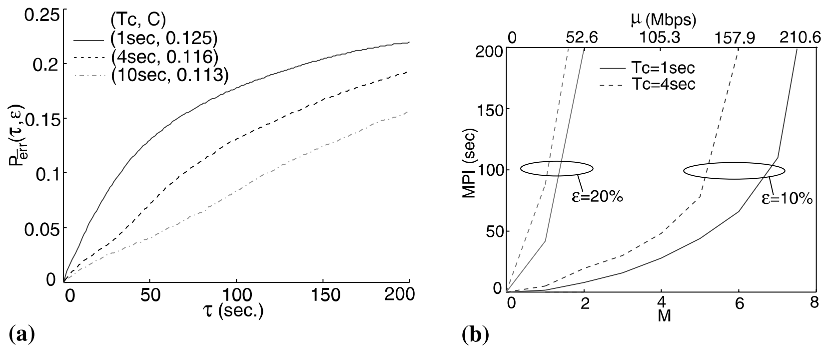

Fig. 10. CMPP-matched Internet trace: (a) steady-state BOSPr, $\varepsilon = 10\%$ (b) MPI with $P_\varepsilon = 0.01$.

plode into the product of the state numbers of all the M sources. To avoid this, the CDF of the aggregate source is first obtained from the convolution of the CDFs of all the M sources, then it is quantified with a reasonable state number N, at the cost of a granularity loss with the resulted rate vector. The CMPP modeling procedure can be done by the SMAQ tool [17].

4.2. Predictability studies for real traffic traces

This section examines traffic predictability for CMPP-matched real traces. Using the Internet traffic as an example, Fig. 9 shows that CMPP and ARMA can capture the PSD of real traces equally well (where the solid line merges with the dashed line), but CMPP has a better match of the CDF than ARMA (where the dashed line merges with the dotted line). In Fig. 10(a), the steady-state BOSPr increases with τ, reminding us of the tradeoff between a large τ and a small prediction error. Fig. 10(b) again confirms the beneficial effect of low-pass filtering and multiplexing on traffic predictability as before.

There are obvious numerical differences between the prediction of CMPP (Tables 4 and 5) and ARMA (Tables 1 and 2). It comes from the modeling change, especially the different matching effect of the traffic tail distribution. In spite of that, the MPI values from both models are approximately at the same scale to upper bound the feasible prediction intervals. By Tables 4 and 5, CMPP analysis shows the same picture about the predictability of single end-system traffic verses

Table 4
CMPP-based MPI (s) for single trace, $P_\varepsilon = 0.01$

ε	T_c (s)	MPEG-1	JPEG	Ethernet	Internet
10%	1	*0.07*	*0.09*	*0.02*	1.8
	4	*0.13*	*0.26*	*0.02*	5.2
	10	*0.14*	*1.04*	*0.03*	*8.4*
20%	1	*0.08*	*0.28*	*0.03*	41.7
	4	*0.26*	*2.40*	*0.05*	88.2
	10	*0.43*	*8.30*	*0.19*	$+\infty$

Table 5
CMPP-based MPI (s) for i.i.d. multiplexed traces, $(P_\varepsilon, \varepsilon) = (0.01, 10\%)$

Load level	T_c (s)	MPEG-1	JPEG	Ethernet	Internet
Mean at	1	$+\infty$	2.8	*0.24*	8.3
OC-1	4	$+\infty$	49.8	*1.20*	19.7
	10	$+\infty$	$+\infty$	15.06	21.3
Mean at	1	$+\infty$	$+\infty$	6.78	65.9
OC-3	4	$+\infty$	$+\infty$	$+\infty$	$+\infty$
	10	$+\infty$	$+\infty$	$+\infty$	$+\infty$

Internet backbone traffic or aggregate end-system sources. Again, the sampling interval greatly affects the assessment.

5. Discussion

Previously we used (BOSPr, BOSP) to measure the prediction cost in terms of the over-subscribed bandwidth resource. Actually there is a symmetric possibility for bandwidth under-subscription to occur. Take a further look at the predictability definition in Section 3.1. The predictor $\hat{Y}(t+\tau)$ there has the same mean value as $Y(t+\tau)$, but a smaller variance. It means that the predictor process is smoother compared to the predicted process, which explains why the predicted rate "peak" tends to be lower than the actual value, but the predicted rate "valley" tends to be higher. This phenomenon is often seen in applications of ARMA prediction. It may upset the network controller who is seeking for an accurate peak rate prediction. For instance, in measurement-based CAC (MCAC), the peak traffic rate in the next control time interval, which is upper bounded by τ, is usually estimated from an observed history with limited length T_m. The result is taken as the future traffic load for CAC purposes. Previous research mainly focused on T_m, as did by [7]. Ref. [9] estimates traffic load for the next control interval T based on the peak rate in the past interval, but T is only empirically fixed. As an improvement, [3] dynamically tunes T, where it is named W, to adapt to the online monitored QoS. Therefore, a peak rate predictability analysis would provide an upper bound of T, and explore the CAC potential in gaining a maximized bandwidth utilization.

However, the above mentioned phenomenon reveals an "asymmetry" embedded in our predictability definition, and shows its limitation in the peak rate case: Traffic valleys contribute more to the total prediction error than peaks. It is natural since predictor tends to over-estimate the rate valley with a larger percentage than the rate peak. In mathematical words, given symmetric $y_r(>\mu)$ and $y_l = 2\mu - y_r$ around the mean value, there are two corresponding components in $P_{\overline{\mathrm{err}}}(\tau, \varepsilon)$:

$$P_{\overline{\mathrm{err}}}^{Y \geqslant y_r}(\tau, \varepsilon) = \Pr[\overline{\mathrm{err}}(\tau) > \varepsilon, Y(t+\tau) \geqslant y_r] = \int\int_{D1} f(x,y)\,\mathrm{d}x\,\mathrm{d}y,$$

$$P_{\overline{\mathrm{err}}}^{Y \leqslant y_l}(\tau, \varepsilon) = \Pr[\overline{\mathrm{err}}(\tau) > \varepsilon, Y(t+\tau) \leqslant y_l] = \int\int_{D2} f(x,y)\,\mathrm{d}x\,\mathrm{d}y,$$

where $f(x,y)$ is the bivariate p.d.f. of the two independent Gaussian variables (x and y) in Fig. 11. The shadowed areas ($D1$ and $D2$) in the figure are circled by the following three lines:

$$\mathrm{L1}:\ y = \frac{(y_r - \mu - \sqrt{\hat{\sigma}_\tau^2}x)}{\sqrt{\sigma^2 - \hat{\sigma}_\tau^2}};$$

$$\mathrm{L2}:\ y = \frac{(y_l - \mu - \sqrt{\hat{\sigma}_\tau^2}x)}{\sqrt{\sigma^2 - \hat{\sigma}_\tau^2}};$$

$$\mathrm{L3}:\ y = \frac{(-\varepsilon\mu - \sqrt{\hat{\sigma}_\tau^2}x)}{\varepsilon\sqrt{\sigma^2 - \hat{\sigma}_\tau^2}}.$$

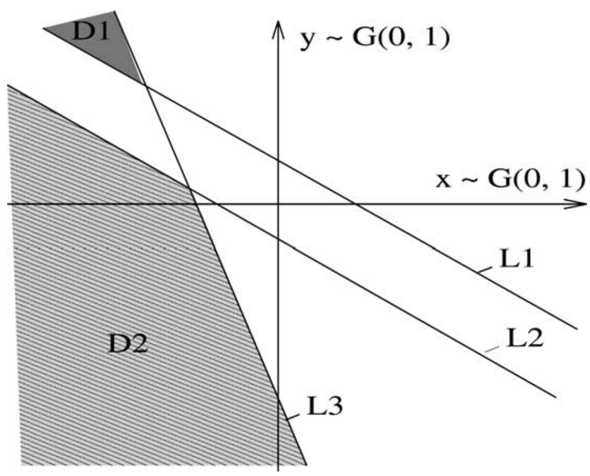

Fig. 11. Asymmetry in $P_{\overline{\mathrm{err}}}(\tau, \varepsilon)$: $P_{\overline{\mathrm{err}}}^{Y \geqslant y_r}(\tau, \varepsilon)$ (D1) is smaller than $P_{\overline{\mathrm{err}}}^{Y \leqslant y_l}(\tau, \varepsilon)$ (D2) despite of $(y_l + y_r)/2 = \mu$.

Of the two components, the former is smaller than the latter albeit y_l and y_s are symmetrically located around μ. This implies more bandwidth over-subscription occurrence when $Y(t+\tau)$ reaches its valley than peak. Therefore, we realize that our predictability definition, by estimating the mean BOSPr over the whole value range of $Y(t+\tau)$, may provide a deviated MPI estimation if only traffic peak rate is the prediction target. In dynamic bandwidth allocation that has a smaller control time-scale, the definition works well since the leftover bandwidth due to the bandwidth over-subscription at this moment might absorb the queued traffic load due to the under-subscription at the last moment. Consequently the two parts in $P_{\overline{\mathrm{err}}}(\tau,\varepsilon)$ offset each other, reflecting a balanced predictability analysis. However, in CAC whose control time-scale might be at buffer non-effective region [14], the asymmetry would deteriorate control performance with alternate in- and out-profile service oscillation. In this scenerio, another definition of BOSPr is comparatively more reasonable:

$$P_{\overline{\mathrm{err}}}(\tau,\varepsilon) \equiv \Pr[\overline{\mathrm{err}}(\tau) > \varepsilon | Y(t+\tau) \geqslant y_r] = \frac{\int\int_{D1} f(x,y)\,\mathrm{d}x\,\mathrm{d}y}{1-\Phi(\frac{y_r-\mu}{\sigma})},$$

where $\Phi(\circ)$ denotes the CDF of $N(0,1)$, and y_r is given as a "peak threshold" to describe the rate region for traffic prediction. Then predictability analysis can be done by applying such a BOSPr in (1).

Different control situation may produce different prediction constraint such as a small bandwidth under-subscription percentage (BUSP) for peak rate prediction, or small BUSP and BOSP at the same time. As a result, traffic prediction should consider the specific requirements from network controller. This argument is illustrated in Fig. 12. The dash lines there imply that the ($P_\varepsilon, \varepsilon$, MPI), as the target of prediction performance metrics, should be specified with reference to the control parameters. Each vertex of the solid-line triangle denotes a metrics measure and its target. Any two vertices can unite together to decide the third one for given traffic process. This diagram outlines our way to view traffic prediction and to do predictability analysis.

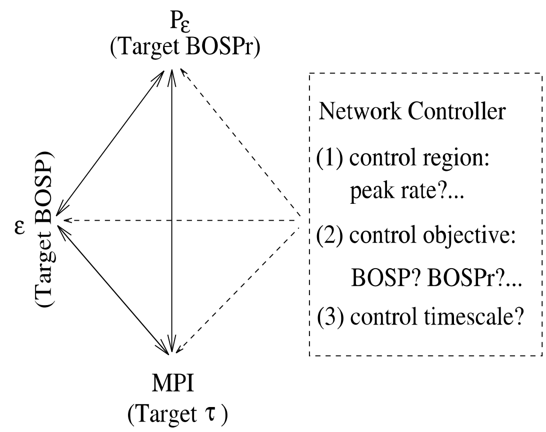

Fig. 12. Guideline to prediction analysis: to evaluate (BOSP, BOSPr, τ) using (P_ε, ε, MPI) as expected by controller.

Actually the above argument is not limited to ARMA prediction. For MMPP, the unsymmetric phenomenon is shown by the non-monotonic $P_{\overline{\mathrm{err}}_i}(\tau,\varepsilon)$ being a function of τ, as found in our simulation. Under this circumstance, predictability analysis should be adjusted similarly. For example, if we intend to predict peak rate process defined by a peak threshold r_t and a given P_ε, a changed index set $\{i\}^* = \{i | r_i \geqslant r_t\}$ should replace the original $\{i\}$ set in (13), so that BOSPr becomes: $P_{\overline{\mathrm{err}}}(\tau,\varepsilon) = \sum_{\{i\}^*} P_{\overline{\mathrm{err}}_i}(\tau,\varepsilon)/|\{i\}^*|$. With this change, other analysis can proceed in the same way.

Previously we discussed the ARMA and MMPP modeling validity in case of self-similar traffic of LRD. We believe that for the limited control timescales in a realistic ATM network of tight QoS constraint, the models derive good approximation. Searching for the best prediction model is beyond our purpose. On the one hand, LRD property may improve the non-trivial short-term prediction, if viewed with 2nd-order property only. On the other hand, LRD traffic can still be very bursty (thus hard to predict), if evaluated by variance coefficient. To make things more complicated, real traffics can be highly non-stationary and of both SRD and LRD components at multiple timescales. Self-similar models of two to three parameters only, though claimed to capture all-scale traffic granularity, need cautious study for online prediction under strict error constraint. With the consideration of the 1st-order statistics (e.g. a long-tail distribution like Pareto), the prediction-based control efficiency and the limited time-scales requirements, self-similar traffic predictability with other models deserves further research. However, both the Gaussian confidence interval and the mean rate estimation in the analysis need to be reconsidered.

6. Conclusion

This paper investigates network traffic predictability in order to explore the potential or optimal bounds of multi-step traffic prediction in traffic engineering. We are especially interested in deriving the upper/lower values of prediction interval or error for representative traffic traces collected from real networks. Having the bound solution is equivalent to achieving the optimal prediction of each given traffic trace. Then it can be used to estimate specific control performance, or select certain control parameters such as the control time-scale or bandwidth utilization target. Our analysis is based on two popular models—ARMA and MMPP—for their available optimal predictors and their popularity in practice.

We believe that the tradeoff between a large MPI and a small prediction error reveals the tradeoff between a selected control time-scale and the corresponding control efficiency. Furthermore, the paper shows that proper traffic measurement (i.e. low-pass filtering) and multiplexing (i.e. aggregating) improves predictability. Both the 1st- and 2nd-order traffic statistics matters in the analysis. Moreover, particular traffic properties like multiple correlation time-scales, large variance coefficient and SRD limit prediction performance. Extensive numerical studies of real traces verify these analytical observations. More specifically, this derives the insights in favor of aggregated, in contrast to per-flow, traffic prediction at limited time-scales. Through an engineering-oriented off-line study given complete traffic knowledge, we would be able to evaluate the online prediction gain and loss, and to estimate the prediction-based control efficiency in practice.

References

[1] A. Adas, Using adaptive linear prediction to support real-time VBR video under RCBR network service model, IEEE/ACM Trans. Network 6 (5) (1998) 635–644.

[2] The Internet Traffic Archive, Bellcore Ethernet Traces, http://www.acm.org/sigcomm/ITA.

[3] C. Casetti, J. Kurose, D. Towsley, An adaptive algorithm for measurement-based admission control in integrated services packet networks, International Workshop on Protocols for High Speed Networks, Sophia Antipolis, 1996.

[4] R.L. Easton, P.T. Hutchinson, R.W. Moncello, R.W. Muise, TASI-E communications system, IEEE Trans. Commun. (1982) 803–807.

[5] Insight into current Internet traffic workloads, Fix-West NAP Trace, http://www.nlanr.net/NA.

[6] M.W. Garrett, W. Willinger, Analysis, modeling and generation of self-similar VBR video traffic, in: SIGCOMM'94, 1994, pp. 268–280, The JPEG traces can be downloaded from ftp://thumper.bellcore.com/pub/vbr.video.trace.

[7] M. Grossglauser, D. Tse, A framework for robust measurement-based admission control, IEEE/ACM Trans. Network 7 (3) (1999) 293–309.

[8] S. Haykin, L. Li, Nonlinear adaptive prediction of nonstationary signals, IEEE Trans. Signal. Process. 43 (2) (1995) 526–535.

[9] S. Jamin, P.B. Danzig, S.J. Shenker, L. Zhang, A measurement-based admission control algorithm for integrated services packet network, SIGCOMM'95, Cambridge, MA, USA, 1995.

[10] S.K. Mitra, J.F. Kaiser (Eds.), Handbook for Digital Signal Processing, Wiley & Sons, New York, 1993.

[11] M.B. Priestley, Spectral Analysis and Time Series, Academic Press, New York, 1992.

[12] O. Rose, Statistical properties of MPEG video traffic and their impact on traffic modeling in ATM systems, Technical Report 101, Institute of Computer Science, University of Wurzburg, 1995. The MPEG-1 traces can be downloaded from ftp://thumper.bellcore.com/pub/vbr.video.trace.

[13] S. Chong, S.Q. Li, J. Ghosh, Predictive dynamic bandwidth allocation for efficient transport of real-time VBR video over ATM, IEEE. JSAC. 13 (1) (1995) 12–23.

[14] Y. Kim, S.Q. Li, Time-scale of interest in traffic management for link bandwidth allocation design, Proc. IEEE Infocom'96 Conference, 1996, pp. 738–748.

[15] J. Ye, S.Q. Li, Folding algorithm: a computational method for finite QBD processes with level-dependent transitions, IEEE Trans. Commun. 42 (2) (1994) 625–639.
[16] S.Q. Li, C. Hwang, Queue response to input correlation functions: continuous spectral analysis, IEEE/ACM. Trans. Network 1 (6) (1993) 678–692.
[17] S.Q. Li, C. Hwang, On the convergence of traffic measurement and queueing analysis: a statistical-match and queueing (SMAQ) tool, IEEE/ACM Trans. Network. (April) (1997) 95–110.
[18] J.D. Pruneski, S.Q. Li, The linearity of low frequency traffic flow: an intrinsic I/O property in queueing systems, Proc. IEEE Infocom'95 Conference, April 1995, pp. 613–623, also to appear in IEEE/ACM Trans. Network.
[19] I. Norros, On the use of fractional Brownian motion in the theory of connectionless networks, IEEE JSAC 13 (6) (1997) 953–962.
[20] T. Tuan, K. Park, Multiple time scale congestion control for self-similar network traffic, Perform. Evaluation 36–37 (1999) 359–386.
[21] W. Leland, M. Taqqu, W. Willinger, D. Wilson, On the self-similar nature of Ethernet traffic (extended version), IEEE Trans. Network 2 (1) (1994).
[22] J. Beran, R. Sherman, M. Taqqu, W. Willinger, Long-range dependence in variable-bit-rate video traffic, IEEE Trans. Network 43 (2/3/4) (1995).
[23] M. Garrett, W. Willinger, Analysis, modeling and generation of self-similar VBR video traffic, SIGCOMM, 1994.
[24] M. Crovella, A. Bestavros, Self-similarity in World Wide Web traffic: evidence and possible causes, IEEE Trans. Network 5 (6) (1997).
[25] D. Heyman, T. Lakshman, What are the implication of long-range dependence for VBR-video traffic engineering, IEEE Trans. Network 4 (3) (1996).
[26] B. Ryu, A. Elwalid, The importance of long-range dependence of VBR video traffic in ATM traffic engineering: myths and realities, ACM Comput. Commun. Rev. 26 (1996) 3–14.
[27] N. Likhanov, R. Mazumdar, Cell loss asymptotics in buffers fed with a large number of independent stationary sources, IEEE INFOCOM Proceedings, 1998.
[28] M. Montgomery, G. de Veciana, On the relevance of time scales in performance oriented traffic characterizations, IEEE INFOCOM Proceedings, San Franciso, CA, 1996.

Aimin Sang was born in Shandong Province, China in 1974. He received his Ph.D. from the Department of Electrical and Computer Engineering, the University of Texas at Austin in May, 2001. His dissertation was focused on measurement-based traffic management for QoS guarantee in multi-service networks, under the supervision of Prof. San-qi Li. He received his M.S. (1996) from Institute of Automation, Chinese Academy of Sciences, under the supervision of Prof. Ru-Wei Dai, President of Chinese Association of Automation. He earned his B.S. (1993) from University of Science and Technology of China (USTC) in Electrical Engineering. He joined Santera System Inc. in May, 2000, where he is now a member of technical staff and firmware engineer and is involved in developing the next-generation multi-service switch (Media Gateway+Media Gateway Controller+Signaling Gateway). He designed and implemented measurement-based CAC algorithm for the SanteraOne system, and finished a series of ATM projects. His research interests include scaleable DiffServ in a MPLS network, cooperative web caching, re-routing and stability issue in (optical) networks, and fundamental issues in measurement-based network resource management.

San-qi Li received his B.S. degree from Beijing University of Posts and Telecommunications, Beijing, China, in 1976, and the M.A.Sc. and Ph.D. degree from the University of Waterloo, Waterloo, ON, Canada, in 1982 and 1985, respectively, all in Electrical Engineering. From 1985 to 1989, he was Associate Research Scientist and Principal Investigator at Center for Telecommunications Research at Columbia University, New York in September 1989, he joined the faculty of the Department of Electrical and Computer Engineering, The University of Texas at Austin, where he is Temple Foundation Endowed Professor. He is also an Honorable Professor at Beijing University of Posts and Telecommunication, China. He has published more than 150 papers in international archival journals and referred international conference proceedings. The main focus of his research has been to develop new analytical methodologies and carry out performance analysis of multimedia service networks, then understand system fundamentals and explore new design concepts. Dr. Li served as a Member of the Techincal Programm Committee for IEEE Infocom Conference since 1988 to 1998. From 1995 to 1997, he served as an Editor for IEEE/ACM Transaction on Networking.